Mechanism of Flavin Reduction in Class 2 Dihydroorotate Dehydrogenases†

Rebecca L. Fagan, Maria N. Nelson, Paul M. Pagano, and Bruce A. Palfey*

Department of Biological Chemistry, University of Michigan Medical School, Ann Arbor, Michigan 48109-0606

Received May 9, 2006; Revised Manuscript Received October 17, 2006

ABSTRACT: Dihydroorotate dehydrogenases (DHODs) oxidize dihydroorotate (DHO) to orotate using the FMN prosthetic group to abstract a hydride equivalent from C6 and a protein residue (Ser for Class 2 DHODs) to deprotonate C5. The fundamental question of whether the scission of the two DHO C−H bonds is concerted or stepwise was addressed for two Class 2 enzymes, those from *Escherichia coli* and *Homo sapiens*, by determining kinetic isotope effects on flavin reduction in anaerobic stopped-flow experiments. Isotope effects were determined for the *E. coli* enzyme at two pH values below a previously reported pK_a controlling reduction [Palfey, B. A., Björnberg, O., and Jensen K. F. (2001) *Biochemistry 40*, 4381−4390] and were about 3-fold for DHO labeled at the 5-position, about 4-fold for DHO labeled at the 6-position, and about 6−7-fold for DHO labeled at both the 5- and 6-positions. These isotope effects are consistent with either a stepwise oxidation of DHO or a concerted mechanism with significant quantum mechanical tunneling. At a pH value above the pK_a controlling reduction, no isotope effect was observed in *E. coli* DHOD for DHO deuterated at the 5-position (the proton donor in the reaction). This is consistent with a stepwise reaction; above the (kinetic) pK_a, the deprotonation of C5 is fast enough that it does not contribute to the observed rate constant and, therefore, is not isotopically sensitive. All available information points to Ser acting as a component in a proton relay network which allows its transient deprotonation. The *H. sapiens* DHOD also appears to have a pK_a near 9.4 controlling reduction, similar to that previously reported for the *E. coli* enzyme. Similar KIEs were obtained with the *H. sapiens* enzyme at a pH value below the pK_a.

Dihydroorotate dehydrogenases (DHODs[1]) are flavin-containing enzymes that catalyze the oxidation of dihydroorotate (DHO) to orotate (Scheme 1), the only redox step in the *de novo* synthesis of pyrimidines. DHODs fall into two broad classes on the basis of sequence (*1*). Class 1 enzymes are cytosolic enzymes that use cysteine as an active site base. This class is further divided into two subclasses, 1A and 1B (*2*, *3*). Class 1A enzymes contain only FMN as a prosthetic group and use fumarate as the oxidizing substrate (*3*). Class 1B enzymes have a second protein subunit that contains an iron−sulfur cluster and an FAD in addition to a subunit that resembles the Class 1A enzymes (*2*). Class 2 enzymes, in comparison, are membrane bound, are oxidized by ubiquinone (*4*), and use a serine as the active site base. Class 1 DHODs are found mostly in Gram-positive bacteria while Class 2 DHODs are found in the majority of Gram-negative bacteria and eukaryotes.

The oxidation of DHO involves both a deprotonation and a hydride transfer, forming the α,β-unsaturated carbonyl moiety of the product orotate. Oxidations that form α,β-unsaturated carbonyl compounds (or the reverse reaction) are catalyzed by a number of flavin-containing enzymes (*5*). In reactions such as these, the slightly acidic proton α to the carbonyl (for DHOD, the C5 *pro S* hydrogen of DHO (*6*)) is removed by an active site base (either Ser in Class 2 enzymes or Cys in Class 1 enzymes) and the β-hydrogen (for DHOD, the hydrogen on C6 of DHO) is transferred to N5 of the isoalloxazine of the flavin as a hydride or hydride equivalent. Structures of such enzymes show that N5 of the flavin is in van der Waals contact with the hydride donor/acceptor and the active site base (or acid) is positioned correctly for deprotonation/protonation at the site α to the carbonyl. Residues with hydrogen-bonding capabilities are generally present in the active site to stabilize possible charge development. With four asparagines and a threonine or serine providing hydrogen bonds of potential catalytic importance, DHODs possess these characteristics (Figure 1), making them excellent model systems for investigating mechanisms in flavin−enone reactions.

Scheme 1

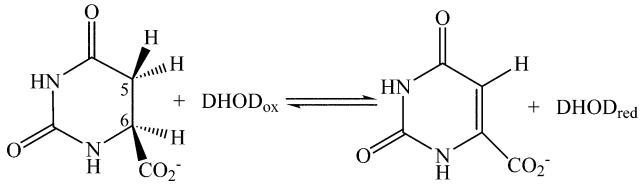

During the oxidation of DHO, the two C−H bonds of DHO could break at the same time in a concerted mechanism, or they could break sequentially in a stepwise mechanism. To address the question of whether the oxidation of DHO is stepwise or concerted, kinetic isotope effects on flavin reduction were determined in anaerobic stopped-flow

† This work was supported by NIH Grant GM61087. R.L.F. was supported by NIGMS training grant GM07767.

* To whom correspondence should be addressed. Phone: (734) 615-2452. Fax: (734) 764-3509. E-mail: brupalf@umich.edu.

[1] Abbreviations: DHOD, dihydroorotate dehydrogenase; DHO, dihydroorotate; OA, orotate; KIE, kinetic isotope effect; KPi, potassium phosphate buffer.

10.1021/bi060919g CCC: $33.50
Published on Web 11/24/2006

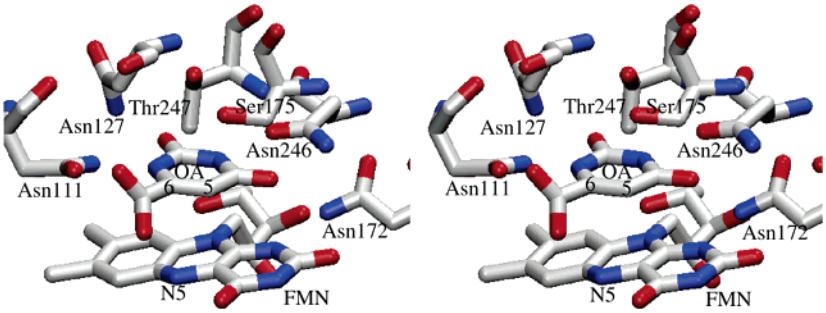

FIGURE 1: Stereoview of the active site of *E. coli* DHOD. Orotate (OA) is stacked against the flavin with N5 of FMN, the site of hydride transfer, in van der Waals contact with C6 of orotate. Ser175, the active site base, is positioned correctly for deprotonation of C5. Four Asn side chains and one Thr side chain are present in the active site and could potentially help to stabilize the formation of a charged intermediate.

experiments using DHO deuterated at the 5-position, the 6-position, or both the 5- and 6-positions. Isotope effects were determined for two Class 2 enzymes: those from *Escherichia coli* and from *Homo sapiens*. We found that if hydrogen tunneling effects are small, Class 2 enzymes oxidize DHO in a stepwise mechanism.

EXPERIMENTAL PROCEDURES

The expression plasmid for *E. coli* DHOD was the gift of Professor Kaj Frank Jensen (University of Copenhagen). The expression plasmid for a construct of the *H. sapiens* enzyme with a deletion of the N-terminal membrane-inserting hydrophobic sequence (residues 1−29) was a gift from Professor Lizbeth Hedstrom (Brandeis University). Dihydroorotate dehydrogenases from *E. coli* and *H. sapiens* were overexpressed and purified according to published procedures (*7*, *8*). Deuterium-labeled DHO was synthesized from L-dihydroorotic acid (Sigma) or orotic acid (Aldrich) according to the procedures of Pascal and Walsh (*6*), and characterized by mass spectrometry and ^{1}H-NMR. Proton NMR showed less than 4% contamination by protium in all compounds synthesized. Absorbance spectra were obtained using a Shimadzu UV-2501PC scanning spectrophotometer. Stopped-flow experiments were performed at 4 °C using a Hi-Tech Scientific KinetAsyst SF-61 DX2 stopped-flow spectrometer controlled by KinetAsyst 3 software for Windows. Enzyme solutions for rapid reaction studies were made anaerobic in glass tonometers by repeated cycles of evacuation and equilibration over an atmosphere of purified argon (*9*). Substrate solutions were made anaerobic by bubbling solutions with purified argon within the syringes that were to be loaded onto the stopped-flow instrument. The pH dependence of the reductive half-reaction of the human DHOD was studied using buffers ranging from pH 6 to 11.3. The enzyme, in 3 mM KPi, 150 mM KCl, 10% glycerol, 0.1 mM EDTA, pH 6.66, was mixed with 0.1 M buffer (KPi pH 6−7.7; Tris-HCl pH 7.8−8.9; CHES pH 9.0−10.2; CAPS pH 10.3−11.3) at the pH of interest which also included 150 mM KCl, 10% glycerol, 0.1 mM EDTA and contained concentrations of DHO ranging from 0 to 4 mM (0 to 2 mM final concentrations after mixing). Control experiments showed that the rate of equilibration of the enzyme with the new pH of the buffer after the pH jump was much more rapid than the reduction reaction. Kinetic isotope effects on the *E. coli* enzyme were studied at three pH values: pH 6.5, 8.5, and 10.5. At pH 6.5 and 8.5, the enzyme in 0.1 M buffer (KPi at pH 6.5 and Tris-HCl at pH 8.5) was mixed with solutions of DHO ranging from 0 to 0.2 mM (~40K_d) in the same buffer. At pH 10.5, the *E. coli* enzyme in 10 mM glycine was mixed with solutions of DHO (up to 4 mM), which was made anaerobic in distilled H_2O (pH ~6.5) to remove the possibility of base-catalyzed exchange at the C5 position of DHO (*10*). The KIE for the *H. sapiens* enzyme was determined at pH 8.0 in 0.1 M Tris-HCl, 150 mM KCl, 10% glycerol, 0.1 mM EDTA. Absorbance traces were fit to either two or three exponentials depending on whether biphasic or triphasic exponential decays were observed, using KinetAsyst 3 (Hi-Tech Scientific), pro Fit (Quantum Soft), or Program A (Rong Chang, Chung-Jin Chiu, Joel Dinverno, and David P. Ballou, University of Michigan). In all cases, the apparent rate constant for reduction was determined by fitting directly to eq 1 using KaleidaGraph (Synergy Software). Here, k_{red}

$$k_{obs,1} = \frac{k_{red}[DHO]}{K_d + [DHO]} \quad (1)$$

is the rate constant of flavin reduction and K_d is the apparent dissociation constant of DHO. The pH dependence of the rate constant for the reduction of the human DHOD was fit to eq 2 using pro Fit (Quantum Soft), where $k_{red,max}$ represents the reduction rate constant at the high-pH extreme.

$$\log k_{red} = \log\left[\frac{10^{-pH}k_{red,max}}{10^{-pK_a} + 10^{-pH}}\right] \quad (2)$$

Kinetic traces were simulated by using a fourth-order Runge−Kutta algorithm implemented in Berkeley Madonna X, version 8.1β15.

RESULTS

Reduction of H. sapiens DHOD. The kinetics of the reductive half-reaction of the Class 2 DHOD from *H. sapiens* were studied at various pH values in anaerobic stopped-flow experiments. Enzyme was mixed with DHO in the absence of an oxidizing substrate so that only the reductive half-reaction could occur. DHO binds to the human enzyme in the dead-time of the stopped-flow instrument, causing a large red shift in the FMN absorbance peak. This shift—from 456 to 470 nm—seen in the human enzyme−substrate complex is similar to that previously observed for DHOD−DHO or DHOD−orotate complexes in the *E. coli* enzyme as well as in Class 1A DHODs from both *Lactococcus lactis* and *Enterococcus faecalis* (*1*, *11*−*13*). After the formation of the enzyme−substrate complex, flavin absorbance decreases rapidly as DHO is oxidized in the first observable kinetic

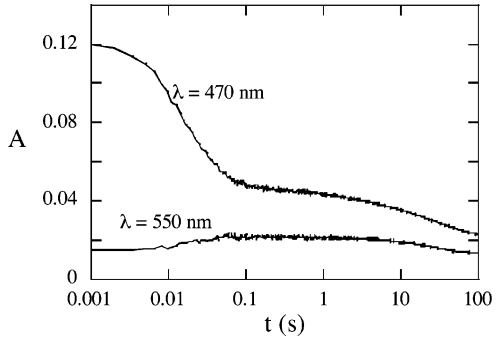

FIGURE 2: Reduction of *H. sapiens* DHOD. Anaerobic DHOD (11 μM after mixing) was mixed with DHO (final concentration 2 mM) in 0.1 M Tris, pH 8.7, at 4 °C in a stopped-flow spectrometer. Note that reaction traces are displayed on a logarithmic time scale. At 470 nm, flavin reduction is seen as a rapid decrease in absorbance and orotate dissociation is seen as a small and slow decrease in absorbance. At 550 nm, flavin reduction is seen as an increase in absorbance while orotate dissociation is seen as a decrease in absorbance.

Scheme 2

$$DHOD_{ox} + DHO \underset{}{\overset{\text{very fast}}{\rightleftharpoons}} DHOD_{ox}\bullet DHO \rightleftharpoons DHOD_{red}\bullet OA \overset{\text{slow}}{\rightleftharpoons} DHOD_{red} + OA$$

$$DHOD_{red} + DHO \rightleftharpoons DHOD_{red}\bullet DHO$$

dead-end complex

phase (Figure 2). The reduced enzyme−orotate complex formed in this reaction has a charge-transfer band extending to long wavelengths, which indicates stacking of orotate with the reduced FMN. This is seen as an increase in absorbance at 550 nm (Figure 2). The loss of this charge-transfer absorbance, corresponding to product dissociation, occurs slowly. Between these two phases, we occasionally observed a small decrease at 470 nm (less than 10% of the change corresponding to the main phase of flavin reduction) which was not observed at 550 nm. It is not clear what this phase represents, but we speculate that it was caused either by the consumption of a small amount of contaminating oxygen in an oxidase turnover reaction or by a small amount of damaged enzyme. Regardless of its origin, this reaction phase was always well-resolved—generally at least an order of magnitude slower than the main phase of flavin reduction and one or two orders of magnitude faster than orotate dissociation—so that it did not interfere with the analysis of the other phases.

Absorbance traces collected at 470 nm were fit to three exponentials, and traces collected at 550 nm were fit to two exponentials. The observed rate constants obtained for the first phase in these fits describe the time-dependence of the reaction of the DHO-oxidized enzyme complex to form the orotate-reduced enzyme complex, modulated by the fraction of enzyme that has DHO bound (a function of the K_d). At saturating DHO, the observed rate constant will depend only on the reaction leading from the DHO complex to the orotate complex. At both wavelengths investigated, the observed rate constant of the first phase varied hyperbolically with DHO concentration, allowing the overall rate constant for flavin reduction (k_{red}) to be determined. At pH 8.7 and 4 °C, k_{red} was 52 ± 1 s^{-1} and a K_d for DHO of 31 ± 2 μM was found.

It is important to be clear about the meaning of k_{red}. The equilibrium of the overall reduction reaction lies far toward reduced flavin (*11*); therefore, if the reaction occurs in a single step (a concerted reaction), the reverse reaction is negligibly slow and the observed rate constant at saturation will represent the rate constant for flavin reduction. If the reaction is stepwise, then the limiting observed rate constant will be a function of the rate constants of each step. These key mechanistic issues are addressed by the KIE experiments described in a later section.

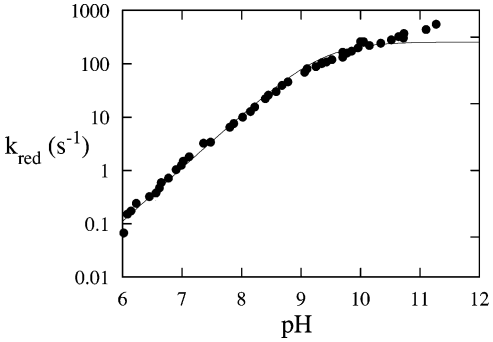

FIGURE 3: pH dependence of *H. sapiens* DHOD reduction. The limiting rate constants for reduction (k_{red}) were obtained from pH-jump stopped-flow experiments as described in the text. The curve represents the best fit to eq 2, giving a pK_a value of 9.36 ± 0.02 and maximum rate constant for flavin reduction at high pH of 255 ± 10 s^{-1}. However, it is clear that the data deviate significantly at the highest pH values.

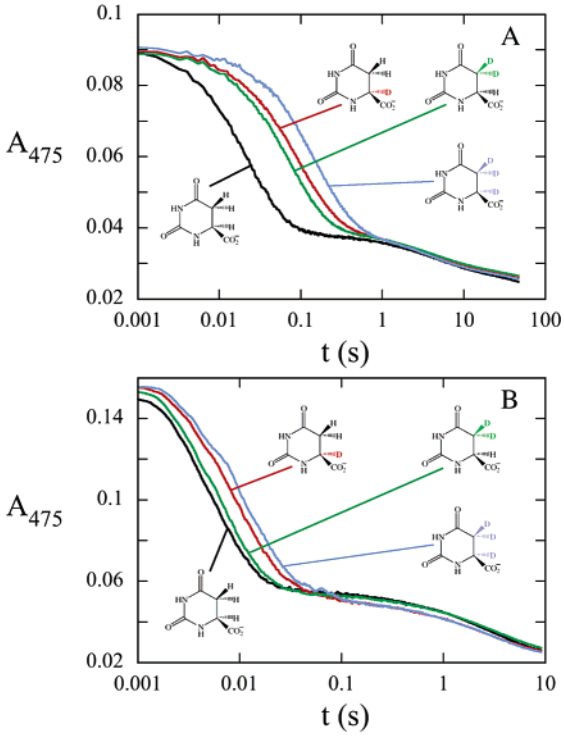

FIGURE 4: Reduction of *E. coli* DHOD with labeled and unlabeled DHO. (A) Anaerobic DHOD (final concentration 7.41 μM) was mixed with anaerobic substrate (final concentration 200 μM) at 4 °C in a stopped-flow spectrometer at pH 8.5. (B) Anaerobic DHOD (final concentration 13.3 μM) was mixed with anaerobic substrate (final concentration 200 μM) at pH 10.5. Note that the reaction traces, collected at 475 nm, are shown on a logarithmic time scale. Protio-DHO is shown in black, 5,5-$^2H_2$ DHO is shown in green, 6-^{2}H DHO is shown in red, and 5,5,6-$^2H_3$ DHO is shown in periwinkle.

The observed rate constant for the dissociation of the charge-transfer complex, observed at 550 nm, decreased from a value of ~0.2 s^{-1} at low DHO concentrations (3.75 μM) to a limiting value of ~0.023 s^{-1} at high DHO concentrations

Table 1: Reduction Rate Constants and KIEs for *E. coli* DHOD[a]

	pH 6.5		pH 8.5		pH 10.5	
compound	k_{red} (s^{-1})	KIE	k_{red} (s^{-1})	KIE	k_{red} (s^{-1})	KIE
DHO	0.882 ± 0.004		40 ± 2		242 ± 3	
5,5-$^2H_2$ DHO	0.276 ± 0.005	3.2 ± 0.2	14 ± 0.2	2.9 ± 0.2	221 ± 2	1.09 ± 0.02
6-^{2}H DHO	0.203 ± 0.007	4.4 ± 0.3	11.2 ± 0.1	3.6 ± 0.2	127 ± 3	1.90 ± 0.07
5,5,6-$^2H_3$ DHO	0.120 ± 0.007	7.4 ± 0.7	6.8 ± 0.1	5.9 ± 0.4	121 ± 2	1.99 ± 0.09

[a] Rate constants were obtained from the value at saturating DHO concentration as explained in Experimental Procedures. The highest concentration of DHO used (after mixing) was 200 μM at pH 6.5 and 8.5 (more than 40 times K_d) and 4 mM at pH 10.5 (more than 80 times K_d).

(500 μM) (data not shown). This behavior was seen in experiments using enzyme concentrations ranging from 6.9 μM to 12.6 μM. The decrease in observed rate constant with increasing DHO concentration is diagnostic for a unimolecular reaction step—in this case orotate release—followed by a bimolecular reaction: binding of DHO to free reduced enzyme (Scheme 2). Interpreting the observed rate constant extrapolated to zero DHO is potentially complex because the regime of pseudo-first-order kinetics is left. However, the value of the observed rate constant as DHO concentration becomes high, $\sim$0.023 s^{-1}, represents the rate constant for orotate dissociation. Thus the reduced human enzyme also makes a tightly bound orotate complex like that previously reported for the *E. coli* enzyme (*11*), where orotate dissociation is only possible to a significant extent in the presence of a high concentration of DHO, which acts as a competing ligand.

The rate constant for flavin reduction in the human enzyme was determined for pH values ranging from 6 to 11.3 in pH-jump stopped-flow experiments, where weakly buffered anaerobic enzyme solutions were mixed with anaerobic solutions of DHO containing concentrated buffer. Control experiments showed that the enzyme equilibrated rapidly with the new buffer, giving rates identical to those obtained in reactions starting with enzyme at the target pH. The rate constant for flavin reduction increased with pH from a value of 0.07 s^{-1} at pH 6 to about 80 s^{-1} at pH 9 (Figure 3), where there is a break in the log plot, indicating a pK_a. Fitting these data to an expression for k_{red} in which the deprotonation of an ionizable group promotes reduction (eq 2) gave a pK_a value controlling reduction of 9.36 ± 0.02 and a maximum rate constant for reduction of 255 ± 10 s^{-1}. However, the data deviate markedly from the calculated curve at high pH values, indicating a more complex situation. In comparison, the reduction rate constant of the *E. coli* DHOD has been previously studied and was found to behave more simply; it increased with pH to a similar limiting value (360 ± 20 s^{-1}) above a pK_a of 9.5 (*11*) but did reach a plateau. The dissociation constant of DHO from the human enzyme also varied with pH, increasing from a value of 4.6 μM at pH 7.2 to a value of 330 μM at pH 11.3 (data not shown), with no plateau, suggesting that deprotonation of the amide nitrogen of DHO or the deprotonation of Lys 100 (which forms a salt bridge to the pyrimidine) prevents binding. This behavior is qualitatively similar to that of the *E. coli* enzyme (*11*).

Kinetic Isotope Effects on Flavin Reduction. Because the oxidation of DHO might occur via either concerted or stepwise mechanisms, double kinetic isotope effects were measured to determine which mechanism is operational in our model Class 2 DHODs. Anaerobic stopped-flow experiments were conducted by mixing *E. coli* DHOD with DHO in the absence of an oxidizing agent, ensuring that only the reductive half-reaction would occur. Reactions were carried out at 4 °C, which slowed the reduction sufficiently so that it could be observed. Similar to the human enzyme, DHO binding caused a large red shift in the flavin absorbance spectrum of *E. coli* DHOD as previously reported (*11*). Reactions were monitored at 475 nm and were biphasic. The fast reaction phase, corresponding to flavin reduction, was over within $\sim$100 ms, while product dissociation was much slower. Absorbance traces at 475 nm (Figure 4) were fit to two exponentials. Observed rate constants for reduction varied hyperbolically with DHO concentration, allowing k_{red} to be determined. Kinetic isotope effects (KIEs) were obtained by dividing the k_{red} determined for protio-DHO by the k_{red} determined for deuterated DHO.

Table 2: Reduction Rate Constants and KIEs for *H. sapiens* DHOD at pH 8.0[a]

compound	k_{red} (s^{-1})	KIE
DHO	10.9 ± 0.1	
5,5-$^2H_2$ DHO	2.62 ± 0.04	4.15 ± 0.09
6-^{2}H DHO	2.88 ± 0.04	3.77 ± 0.08
5,5,6-$^2H_3$ DHO	1.37 ± 0.02	8.0 ± 0.2

[a] Rate constants were obtained from the value at saturating DHO concentration as explained in Experimental Procedures. The highest concentration of DHO used was 200 μM after mixing (more than 40 times K_d).

KIEs were determined for the *E. coli* DHOD at two pH values below the pK_a of 9.5 previously observed for reduction (*11*). At pH 6.5, using 5,5-$^2H_2$ DHO, a KIE of 3.2 ± 0.2 was found (Table 1), and a KIE of 4.4 ± 0.3 was obtained using 6-^{2}H DHO. The double KIE determined using 5,5,6-$^2H_3$ DHO was found to be 7.4 ± 0.7. Similar values were obtained at pH 8.5 (Table 1). Interestingly, at pH 10.5, above the previously observed pK_a ($\sim$9.5) for the *E. coli* enzyme (*11*), essentially no KIE (1.09 ± 0.02) was observed using 5,5-$^2H_2$ DHO, although the KIEs observed using either 6-^{2}H DHO or 5,5,6-$^2H_3$ DHO were both about 2-fold. No isotope effect was seen on the rate of charge-transfer disappearance at any pH studied, consistent with the assignment of this phase as the dissociation of orotate (Figure 4; data found in Supporting Information). Significant kinetic isotope effects were also observed for the *H. sapiens* enzyme at pH 8.0 (Table 2), similar to those observed for the *E. coli* enzyme at both pH 6.5 and 8.5, with values for both 5,5-$^2H_2$ DHO and 6-^{2}H DHO of around 4-fold and for 5,5,6-$^2H_3$ DHO of around 8-fold. Rate constants obtained for all phases can be found in the Supporting Information.

Deuterium isotope effects were also used to determine whether DHO was a "sticky" substrate for the *E. coli* enzyme. If the oxidation of DHO were much faster than dissociation

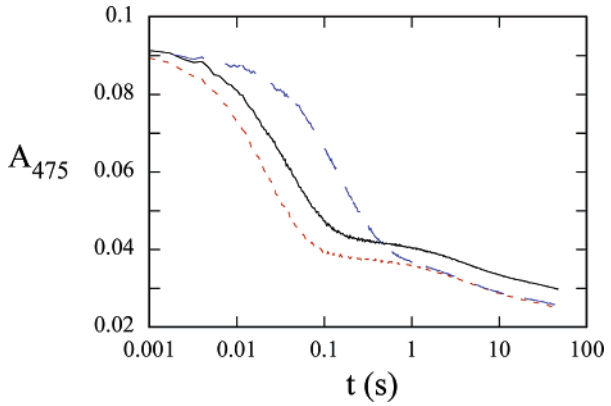

FIGURE 5: *E. coli* DHOD (7.4 μM) was mixed with 200 μM DHO (red - - -), 200 μM 5,5,6-$^2H_3$ DHO (blue — — —), or a mixture of 200 μM DHO and 200 μM 5,5,6-$^2H_3$ DHO (black —). All concentrations are for solutions after mixing. Note the logarithmic time scale. Flavin reduction by the isotopic mixture occurs in one phase.

from the oxidized enzyme (i.e., if it were a "sticky" substrate), then an equimolar mixture of labeled and unlabeled DHO would form equal populations of complexes with and without deuterium, and each of these would subsequently react faster than DHO dissociation. In such a situation, two phases of flavin reduction—a fast phase corresponding to protio-DHO and a slow phase corresponding to deutero-DHO—would be observed. On the other hand, if DHO dissociated rapidly compared to its reaction with FMN, then only one phase of flavin reduction would be observed because oxidized enzyme would continually equilibrate with the pool of isotopically mixed DHO. When *E. coli* DHOD was mixed with a solution containing 400 μM protio-DHO and 400 μM 5,5,6-$^2H_3$ DHO at pH 8.5, 4 °C, only one reaction phase was observed for flavin reduction (Figure 5), demonstrating that DHO dissociates rapidly compared to flavin reduction. Simulations showed that two phases would be observed for a commitment factor (the ratio of the reduction rate constant to the DHO dissociation rate constant) as low as 0.45 when mixing DHOD with a solution of both protio- and 5,5,6-$^2H_3$ DHO.

DISCUSSION

All DHODs oxidize DHO to orotate by transferring a hydride or a hydride equivalent from C6 of DHO to the flavin and by deprotonating C5 of DHO with an enzyme side-chain. An issue central to the mechanism is the timing of the two C−H bond cleavages. These could be concerted, with both C−H bonds breaking in a single transition state, or stepwise, with each C−H bond breaking in separate transition states. Double kinetic isotope effects can be used to distinguish between concerted or stepwise mechanisms for flavin reduction. The Rule of the Geometric Mean states that, in the absence of large quantum effects, perturbations to a partition function caused by isotopic substitutions at a particular site are independent of isotopic substitutions at other sites (*14*). Therefore, if both C−H bonds break in a concerted mechanism (i.e., a single transition state), then the product of the two single isotope effects (obtained by comparing 5,5-$^2H_2$ DHO and 6-^{2}H DHO with the protio-DHO) will equal the observed double KIE (obtained by comparing 5,5,6-$^2H_3$ DHO with the protio-DHO). Below the observed pK_a for reduction of 9.5 in the *E. coli* enzyme (*11*), the product of the two single-site KIEs is much greater than the KIE measured for 5,5,6-$^2H_3$ DHO (Table 3). Therefore, the Rule of the Geometric Mean is not obeyed; *if quantum mechanical tunneling is not significant*, the mechanism of flavin reduction is stepwise.

Table 3: Analysis of KIEs

pH	5,5-$^2H_2$ DHO	6-^{2}H DHO	predicted double KIEs[a]	5,5,6-$^2H_3$ DHO
		E. coli		
6.5	3.2 ± 0.2	4.4 ± 0.3	13.9 ± 1.8	7.4 ± 0.7
8.5	2.9 ± 0.2	3.6 ± 0.2	10.5 ± 1.3	5.9 ± 0.4
10.5	1.09 ± 0.02	1.90 ± 0.07	2.1 ± 0.1	1.99 ± 0.09
		H. sapiens		
8.0	4.15 ± 0.09	3.77 ± 0.08	15.5 ± 0.6	8.0 ± 0.2

[a] The Rule of the Geometric Mean predicts that, in the absence of quantum effects, the double KIE will be given by the product of the two single KIEs (*14*).

An alternate interpretation of our KIE data is that the oxidation of DHO is concerted but that there is a significant contribution from hydrogen tunneling. If the cleavage of each C−H bond is coupled to the other by significant tunneling, then substituting one hydrogen with deuterium will impair the ability of both hydrogens to tunnel. Isotopic substitution at the second site will, therefore, have a smaller additional impact on the rate when the first site is already substituted with deuterium, and the Rule of the Geometric Mean will not be obeyed, as observed with our results.[2] Our data do not address the possibility of tunneling in hydrogen transfer. Quantum mechanical tunneling sometimes causes very large isotope effects, but the KIEs observed here were not unusually large, so that by this criterion, tunneling need not be invoked. However, there are numerous instances of tunneling that do not exhibit unusually large KIEs, so that the magnitude of the KIE is not a decisive criterion (*15*). Therefore, in the absence of other data, no conclusion can be drawn yet concerning the importance of quantum mechanical tunneling in the reduction of the Class 2 DHODs.

If the oxidation of DHO by Class 2 DHODs is actually stepwise, two reaction phases for flavin reduction in the stopped-flow experiments might be expected. However, only one phase of reduction was observed, i.e., no spectral intermediates or lags were detected during the reaction. This is not inconsistent with behavior possible for a two-step reversible reaction sequence. If the net rate through the first kinetic step is significantly slower than that through the second step, no intermediates would be visible and the process would appear as a single exponential. One detailed example of a model calculation is given in the Supporting Information.

Our kinetic data do not allow the determination of the order of bond-breaking in a two-step oxidation of DHO, i.e., deprotonation followed by hydride transfer or vice versa (Figure 6), and the published crystal structures do not provide a basis for making this distinction either. If deprotonation at

[2] It is also worth noting that the possibility of tunneling need not be limited to a concerted reaction. In the putative stepwise mechanism described above, hydrogen tunneling would also be possible in one or both of the transition states. However, such a scenario would not alter the interpretation.

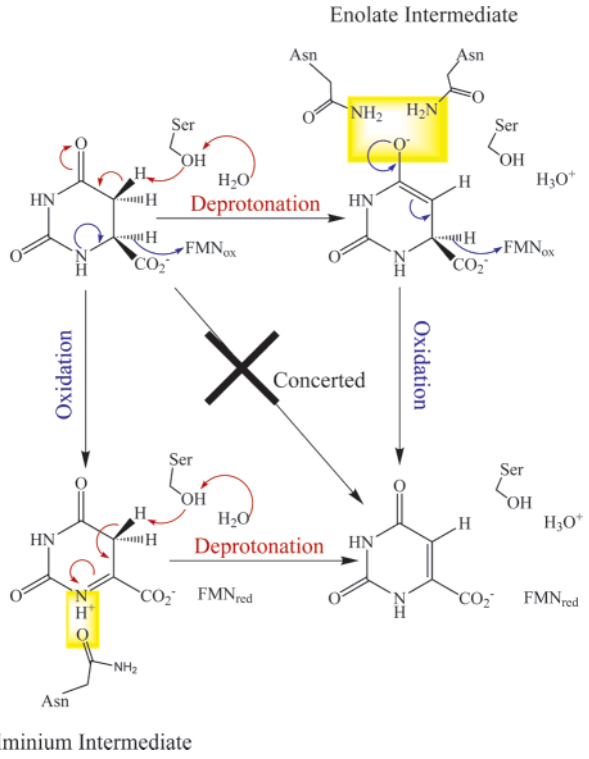

FIGURE 6: Possible mechanisms of DHO oxidation in the absence of tunneling by Class 2 DHODs. Without tunneling, a concerted oxidation of DHO (upper-left corner) to orotate (lower-right corner) is not compatible with our data, but two possible stepwise mechanisms are still possible. If deprotonation precedes hydride transfer, then an enolate intermediate would form that could be stabilized by two conserved asparagines. If hydride transfer (oxidation) precedes deprotonation, an iminium intermediate would form that could hydrogen bond with another conserved asparagine. Note that in both mechanisms, the active site base (Ser) is a component in a proton relay system allowing the transient generation of the alkoxide (not shown) even at pH values below its pK_a. Deprotonation is shown by red arrows, and oxidation is shown by blue arrows. Hydrogen bonds that could stabilize each intermediate are highlighted by yellow boxes.

C5 occurs first, then the reaction would proceed via an enolate intermediate which could be stabilized through hydrogen bonds in the active site. Two conserved Asn side-chains (172 and 246 in the *E. coli* enzyme) are ideally positioned within hydrogen-bonding distance of the O on C4 of the pyrimidine (Figure 1) (*16*). These residues could stabilize the negative charge that would form on this O in a manner similar to the oxyanion "hole" of serine proteases. The other possible order of bond cleavage—hydride transfer from C6 to the flavin followed by deprotonation at C5—leads to an iminium intermediate. An Asn residue (111 in the *E. coli* enzyme) is located within hydrogen-bonding distance of N1 of DHO (Figure 1) (*16*) and could stabilize this intermediate.

The acid/base chemistry necessary in Class 2 DHODs has presented a dilemma. The base that deprotonates C5 of DHO is Ser (Ser 175 in the *E. coli* enzyme and Ser 215 in the human enzyme). The side-chain of free Ser has a high pK_a (~13.6) (*17*), but the pK_a observed for reduction of the Class 2 DHODs is ~9.5. This is too low to be the thermodynamic pK_a for an unactivated Ser residue. However, crystal structures show that, in Class 2 DHODs, the environment of the Ser is somewhat hydrophobic and no residues such as His are nearby to activate the Ser (*16*, *18*). It was suggested that the Ser was activated by a hydrogen bond to a water molecule that is in turn hydrogen bonded to the OH of a Thr residue and stacked on the aromatic ring of a Phe residue (*16*, *18*). These residues are highly conserved in Class 2 DHODs. However, this arrangement, which allows fewer hydrogen bonds to the serine hydroxyl than would be available in bulk water, is unlikely to lower the pK_a. Empirical calculations of the perturbation of the pK_a using the program PROPKA (*19*) agree with this assessment, predicting a slight increase in the pK_a of the base due to the protein environment, rather than a decrease.

A stepwise reaction mechanism for DHO oxidation allows the apparent pK_a of 9.5 to be explained. The lack of a KIE at the C5 position of DHO (the proton donor in the reaction) above the pK_a of reduction shows that this bond cleavage no longer affects the observed rate.[3] At pH 10.5, deprotonation at C5 occurs quickly enough that it no longer contributes to the overall rate of flavin reduction, explaining the lack of an isotope effect using 5,5-$^2H_2$ DHO. Therefore, the observed pK_a of ~9.5 in Class 2 DHODs does not represent the actual thermodynamic pK_a of the active site Ser. Instead, this is a "kinetic" pK_a, shifted "outward" from its thermodynamic value, which might even exceed the standard value of ~13.6 (*17*). If the actual pK_a of the Ser is high, as our data suggest, then the pH dependence of the reaction below the observed pK_a is a result of the variation in the fraction of alkoxide present. The rate of reduction extrapolates to zero (within experimental error) at low pH, suggesting that the neutral Ser side chain does not promote reduction at any detectable rate. The fraction of enzyme that was reduced by DHO did not vary with pH—it reduced completely, even at low pH values—indicating that the alkoxide form of the Ser side chain could be generated from within the DHO complex. Possible proton relay networks allowing the deprotonation of the active site Ser are evident in the structures of Class 2 DHODs. Crystal structures of Class 2 enzymes show that the Ser is accessible to the solvent through a short tunnel (Figure 7), although the carbonyl oxygen of the serine residue blocks direct solvent access and would have to move to allow proton transfer. Alternatively, a network of hydrogen bonds formed by the active site serine, an internal water, and threonine (*16*, *18*) communicates directly with the solvent. Therefore, a proton-transfer network responsible for deprotonating DHO is feasible and consistent with all available data.

The question of whether DHO oxidation by DHODs is stepwise or concerted has been addressed previously by steady-state kinetics for other examples of Class 1A, 1B, and 2 enzymes (*6*, *20*, *21*). It was suggested that the Class 2 enzyme from bovine liver mitochondria utilized a concerted mechanism (*21*), which differs from our findings that Class 2 DHODs utilize a stepwise mechanism. We cannot explain

[3] The variation of the KIE with pH for reduction by 6-^{2}H DHO, from 4.4 at pH 6.5 to 1.9 at pH 10.5, should also be noted, indicating additional kinetic complexity masking KIEs at higher pH values. This may indicate that another step, such as a conformational change, becomes coupled to the reduction reaction at high pH, partially masking the isotope effect. Alternatively, the deprotonation of ionizable groups at the active site, such as Lys 66 (in *E. coli*; 100 in human), which hydrogen bonds to the carboxylate of the pyrimidine ligand, Lys 217 (in *E. coli*; 217 in human), which hydrogen bonds to the flavin at N1 and C2O, or N3 of FMN (pK_a ~9.5 in aqueous solution), might change the intrinsic isotope effect for hydride transfer.

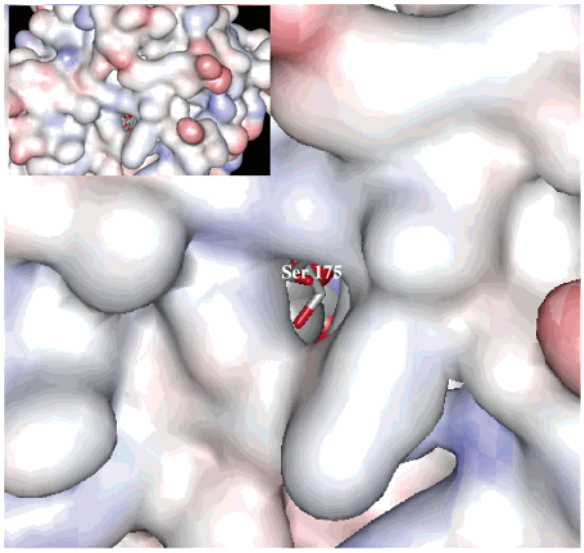

FIGURE 7: Surface of *E. coli* DHOD showing the opening connecting the active site Ser to the solvent. Inset: view of the full protein.

this discrepancy, but note that these authors acknowledged that large errors in their determinations left open the possibility that the mechanism was actually stepwise.

Both the *E. coli* and *H. sapiens* DHODs utilize a stepwise mechanism for flavin reduction (barring large quantum effects), and a kinetic pK_a of ~9.5 is observed in both enzymes. Since all Class 2 enzymes appear to be structurally similar and have high sequence homology, it is likely that these features are true of all Class 2 DHODs. Interestingly, analogous stopped-flow data suggest that Class 1A DHODs utilize a concerted mechanism (R.L.F. and B.A.P., unpublished data) in contrast to an earlier study on the Class 1A enzyme from *Crithidia fasciculata* (*6*). Structures of the Class 1A DHOD from *L. lactis* have been solved (*1*), and they show a high degree of similarity to the structures of the Class 2 enzymes, especially with regard to pyrimidine−protein and flavin−protein interactions. An important difference is that the Class 1A enzymes use a Cys as the active site base. While this might be expected to be responsible for the difference in mechanism, recent studies on base mutants suggest otherwise (R.L.F. and B.A.P., unpublished). The structural basis for the possible mechanistic differences in these two classes of enzymes remains an intriguing question.

ACKNOWLEDGMENT

We thank Professor W. W. Cleland, University of Wisconsin−Madison, and Professor Sharon Hammes-Schiffer, Penn State University, for many helpful discussions.

SUPPORTING INFORMATION AVAILABLE

A detailed explanation of a two-step reaction showing only one phase, along with the rate constants and KIEs determined for orotate release. This material is available free of charge via the Internet at http://pubs.acs.org.

REFERENCES

1. Rowland, P., Nielsen, F. S., Jensen, K. F., and Larsen, S. (1997) The crystal structure of the flavin containing enzyme dihydroorotate dehydrogenase A from Lactococcus lactis, *Structure 5*, 239−252.
2. Nielsen, F. S., Andersen, P. S., and Jensen, K. F. (1996) The B form of dihydroorotate dehydrogenase from Lactococcus lactis consists of two different subunits, encoded by the pyrDb and pyrK genes, and contains FMN, FAD, and [FeS] redox centers, *J. Biol. Chem. 271*, 29359−29365.
3. Nagy, M., Lacroute, F., and Thomas, D. (1992) Divergent evolution of pyrimidine biosynthesis between anaerobic and aerobic yeasts, *Proc. Natl. Acad. Sci. U.S.A. 89*, 8966−8970.
4. Jones, M. E. (1980) Pyrimidine nucleotide biosynthesis in animals: genes, enzymes, and regulation of UMP biosynthesis, *Annu. Rev. Biochem. 49*, 253−279.
5. Palfey, B. A., and Massey, V. (1998) *Comprehensive Biological Catalysis, volume III/Radical Reactions and Oxidation/Reduction*, Academic Press, New York.
6. Pascal, R. A., Jr., and Walsh, C. T. (1984) Mechanistic studies with deuterated dihydroorotates on the dihydroorotate oxidase from Crithidia fasciculate, *Biochemistry 23*, 2745−2752.
7. Björnberg, O., Gruner, A. C., Roepstorff, P., and Jensen, K. F. (1999) The activity of Escherichia coli dihydroorotate dehydrogenase is dependent on a conserved loop identified by sequence homology, mutagenesis, and limited proteolysis, *Biochemistry 38*, 2899−2908.
8. Neidhardt, E. A., Punreddy, S. R., McLean, J. E., Hedstrom, L., and Grossman, T. H. (1999) Expression and characterization of E. coli-produced soluble, functional human dihydroorotate dehydrogenase: a potential target for immunosuppression, *J. Mol. Microbiol. Biotechnol. 1*, 183−188.
9. Palfey, B. A. (2003) Time Resolved Spectral Analysis, in *Kinetic Analysis of Macromolecules* (Johnson, K. A., Ed.) Oxford University Press: New York.
10. Argyrou, A., and Washabaugh, M. W. (1999) Proton Transfer from the C_5-*proR*/*proS* Positions of L-Dihydroorotate: General-Base Catalysis, Isotope Effects, and Internal Return, *J. Am. Chem. Soc. 121*, 12054−12062.
11. Palfey, B. A., Björnberg, O., and Jensen, K. F. (2001) Insight into the chemistry of flavin reduction and oxidation in Escherichia coli dihydroorotate dehydrogenase obtained by rapid reaction studies, *Biochemistry 40*, 4381−4390.
12. Marcinkeviciene, J., Jiang, W., Locke, G., Kopcho, L. M., Rogers, M. J., and Copeland, R. A. (2000) A second dihydroorotate dehydrogenase (Type A) of the human pathogen Enterococcus faecalis: expression, purification, and steady-state kinetic mechanism, *Arch. Biochem. Biophys. 377*, 178−186.
13. Larsen, J. N., and Jensen, K. F. (1985) Nucleotide sequence of the pyrD gene of Escherichia coli and characterization of the flavoprotein dihydroorotate dehydrogenase, *Eur. J. Biochem. 151*, 59−65.
14. Bigelisen, J. (1955) Statistical Mechanics of Isotope Systems with Small Quantum Corrections. I. General Considerations and the Rule of the Geometric Mean, *J. Chem. Phys. 23*, 2264−2267.
15. Basran, J., Masgrau, L., Sutcliffe, M. J., and Scrutton, N. S. (2006) Solution and Computational Studies of Kinetic Isotope Effects in Flavoprotein and Quinoprotein Catalyzed Substrate Oxidations as Probes of Enzymatic Hydrogen Tunneling and Mechanism, in *Isotope Effects in Chemistry and Biology* (Kohen, A. and Limbach, H. H., Eds.) pp 671−689, CRC Press Taylor & Francis Group: Boca Raton, Florida.
16. Nørager, S., Jensen, K. F., Björnberg, O., and Larsen, S. (2002) E. coli dihydroorotate dehydrogenase reveals structural and functional distinctions between different classes of dihydroorotate dehydrogenases, *Structure 10*, 1211−1223.
17. Bruice, T. C., Fife, T. H., Bruno, J. J., and Brandon, N. E. (1962) Hydroxyl group catalysis. II. The reactivity of the hydroxyl group of serine. The nucleophilicity of alcohols and the ease of hydrolysis of their acetyl esters as related to their pKa, *Biochemistry 1*, 7−12.
18. Liu, S., Neidhardt, E. A., Grossman, T. H., Ocain, T., and Clardy, J. (2000) Structures of human dihydroorotate dehydrogenase in complex with antiproliferative agents, *Structure 8*, 25−33.
19. Liu, H., Roberston, A. D., and Jensen, J. H. (2005) Very Fast Empirical Prediction and Rationaliztion of Protein pKa Values, *Proteins 61*, 704-721.
20. Argyrou, A., Washabaugh, M. W., and Pickart, C. M. (2000) Dihydroorotate dehydrogenase from Clostridium oroticum is a class 1B enzyme and utilizes a concerted mechanism of catalysis, *Biochemistry 39*, 10373−10384.
21. Hines, V., and Johnston, M. (1989) Mechanistic studies on the bovine liver mitochondrial dihydroorotate dehydrogenase using kinetic deuterium isotope effects, *Biochemistry 28*, 1227−1234.

BI060919G